



Comparative Analysis Of Air Quality In Urban And Rural Environments Using Satellite And Ground Observations In Nigeria

Adamu Muhammad Kamaludeen¹, Izham Mohamad Yusoff^{2*}

¹School of Distance Education, Universiti Sains Malaysia, 11800 USM Penang, MALAYSIA.
mkamaludeen@student.usm.my,

² Geography Section, School of Distance Education, Universiti Sains Malaysia, 11800 USM Penang,
malaysia.izham@usm.my,

*Corresponding Author: Izham Mohamad Yusoff, School of Distance Education², Universiti Sains Malaysia,
11800 USM Penang, MALAYSIA. malaysia.izham@usm.my,

Abstract

Air pollution poses a persistent environmental and health threat in developing regions, particularly across sub-Saharan Africa, where rapid population growth, industrialization, and inadequate monitoring infrastructure limit effective control. This study employed an integrated approach, combining satellite observations and ground-based measurements, to examine the spatial and temporal dynamics of three major pollutants particulate matter (PM₁₀), ozone (O₃), and nitrogen dioxide (NO₂) across five Northern Nigerian states: Abuja, Bauchi, Plateau, Gombe, and Nasarawa, covering the period from October 2022 to September 2024. Data obtained from MODIS and Sentinel-5P TROPOMI were analyzed alongside local station records to investigate seasonal variations, spatial distribution patterns, and the relationship between satellite and surface observations using Kriging interpolation in ArcGIS.

The findings reveal significant spatial variability and strong seasonal influence. PM₁₀ and PM_{2.5} concentrations peaked during the dry Harmattan season due to intense dust transport, biomass burning, and poor atmospheric dispersion. Abuja and Gombe recorded extreme PM_{2.5} levels of 402.1 µg/m³ and 222.7 µg/m³, respectively far above the WHO guideline of 15 µg/m³ while Plateau consistently exhibited lower concentrations (11–20 µg/m³) due to its elevation and cleaner air mass inflow. Aerosol Optical Depth (AOD) followed a similar distribution, with Gombe showing the highest value (2.803 in February 2024). O₃ levels were highest during the dry months, reaching 282.6 µg/m³ in Abuja, while NO₂ exhibited clear urban–rural contrasts, peaking at 84.2 µg/m³ in Bauchi during December 2022. Correlation analysis indicated moderate satellite ground agreement ($r \approx 0.6$ in Abuja), although satellite data generally overestimated surface concentrations. Kriging interpolation revealed strong spatial autocorrelation (range ≈ 120 km; RMSE ≈ 12 µg/m³) and effectively delineated high-pollution zones around major industrial and traffic corridors.

Overall, the study demonstrates that seasonal meteorology, dust intrusion, and anthropogenic activities are key drivers of air quality fluctuations in selected states in Nigeria. The integration of satellite and ground-based monitoring improves spatial coverage and enhances understanding of pollutant dynamics in data-limited environments. Strengthening monitoring infrastructure, calibrating satellite retrieval algorithms, and implementing emission-control policies are critical for advancing clean-air initiatives and protecting public health across the region.

Keywords: Air pollution, Particulate Matter, Ozone and Nitrogen dioxide

Introduction

Air pollution remains one of the most significant environmental challenges confronting developing nations. According to the World Health Organization (WHO, 2021), over 90% of the global population breathes air that exceeds recommended health-based limits, resulting in millions of premature deaths annually. The situation in sub-Saharan Africa is particularly concerning due to rapid urbanization, population growth, and limited regulatory enforcement (Akinyemi et al., 2023). Northern Nigeria, characterized by both dense urban settlements and expansive rural landscapes, experiences a complex interplay of anthropogenic and natural emission sources. These include vehicular exhaust, industrial operations, biomass burning, and seasonal dust transport from the Sahara Desert (Usman et al., 2022). Three pollutants particulate matter (PM₁₀), ozone (O₃), and nitrogen dioxide (NO₂) have been identified as key indicators of air quality due to their adverse effects on human health and ecosystems (Grange et al., 2021). PM₁₀ particles, due to their small size, can penetrate deep into the respiratory system, causing chronic diseases. Ozone, although beneficial in the stratosphere, is harmful at ground level, contributing to respiratory irritation and vegetation damage. NO₂, primarily produced from combustion processes, plays a central role in the formation of both O₃ and secondary aerosols, amplifying the overall pollution burden. Accurate monitoring of these pollutants is vital for developing effective mitigation strategies. Ground-based instruments provide precise temporal readings but suffer from sparse spatial coverage. Conversely, satellite sensors such as MODIS and Sentinel-5P TROPOMI offer broad spatial insight but represent column-integrated concentrations, potentially overestimating surface exposure (Boersma et al., 2021). Integrating these complementary data sources can improve understanding of air quality dynamics, especially in regions with limited monitoring infrastructure. This study therefore

investigates the spatial and temporal variation of PM₁₀, O₃, and NO₂ between 2022 and 2024 in five Northern Nigerian cities, highlighting seasonal differences and satellite-ground correlations to inform policy and management strategies.

Measurement Techniques

Air quality monitoring relies on two complementary approaches: ground-based observations and satellite remote sensing. Ground-based instruments provide direct, high-accuracy pollutant readings, while satellites offer extensive spatial coverage that captures regional and global pollution trends. Together, they form a comprehensive framework for understanding atmospheric pollution dynamics.

Ground-Based monitoring: Ground stations have long served as the foundation of air quality surveillance, delivering real-time, site-specific data on major pollutants such as nitrogen dioxide (NO₂), ozone (O₃), and particulate matter (PM₁₀). Instruments commonly used include chemiluminescence analyzers for NO₂, beta-attenuation monitors for PM₁₀, and ultraviolet photometers for O₃ (Wahab, Hassan, & Eltahir, 2023). Their precision and temporal resolution make them indispensable for policy formulation and health risk assessments. However, their spatial limitation and high maintenance cost hinder widespread deployment in developing regions, resulting in data gaps across sub-Saharan Africa and parts of Asia (El-Mahdy & Wahba, 2024).

Satellite-Based Monitoring: Satellite remote sensing has transformed global air quality observation by providing consistent, wide-area coverage. The Sentinel-5P TROPOMI instrument, launched in 2017, has become a key advancement for monitoring NO₂ and O₃. It measures tropospheric column densities by analyzing backscattered sunlight, achieving spatial resolutions as fine as 3.5 × 7 km² (Grzybowski et al., 2023). For particulate matter, MODIS and VIIRS sensors estimate surface concentrations indirectly through Aerosol Optical Depth (AOD), a measure of total atmospheric aerosols. Wahab et al. (2023) demonstrated a strong relationship ($R^2 = 0.82$) between MODIS-derived AOD and ground-measured PM₁₀ after meteorological corrections, confirming AOD as a reliable proxy under dry, stable conditions.

Hybrid and AI-Driven Approaches: While satellites provide valuable spatial data, their column-integrated measurements often overestimate surface-level pollution. To address this, researchers increasingly integrate satellite data with ground observations using statistical models and machine learning algorithms. Zhao, Liu, and Xu (2022) combined TROPOMI NO₂ with meteorological and land-use data in a random forest model, improving near-surface estimation ($R^2 = 0.88$). Similarly, Mahmud et al. (2022) employed deep learning to merge satellite and ground datasets in Southeast Asia, reducing mean bias errors by over 20%. Such hybrid models enhance spatial resolution, reduce uncertainty, and are vital for data-scarce regions.

Sensor calibration and retrieval algorithms also play critical roles in accuracy. Jiang, Li, and Zhang (2021) reported that during COVID-19 lockdowns, satellite sensors captured sharp declines in NO₂ and PM₁₀ levels across Asian megacities, validating their responsiveness to emission changes. However, satellite retrieval accuracy remains sensitive to cloud cover, surface reflectivity, and vertical distribution biases, highlighting the need for local validation and algorithm refinement (Grzybowski et al., 2023).

Spatial and Temporal Variations of Air Pollutants

Understanding how pollutants vary across space and time is essential for identifying emission sources, evaluating exposure risks, and guiding control strategies. Spatial patterns reflect emission density, topography, and land use, while temporal trends are shaped by meteorology and human activities.

Nitrogen Dioxide (NO₂): NO₂ is a short-lived pollutant primarily emitted from vehicular exhaust, industrial processes, and fossil fuel combustion. It exhibits strong urban–rural gradients and distinct seasonal cycles. Studies consistently show higher NO₂ levels in urban-industrial corridors compared to rural areas (Zhao et al., 2022). For example, Grzybowski et al. (2023) found that NO₂ concentrations in Poland’s industrial belt were up to three times higher than surrounding rural areas. Ojo, Suleiman, and Bala (2023) observed similar patterns across African cities using Sentinel-5P data, with dry-season peaks caused by reduced atmospheric mixing and increased human activity.

Temporally, NO₂ displays weekly and seasonal cycles driven by traffic volume and meteorology. Mahmud et al. (2022) reported weekday peaks linked to rush-hour traffic and winter maxima associated with temperature inversions that trap pollutants near the surface. During summer, enhanced photochemical activity leads to NO₂ depletion as it participates in ozone formation. These fluctuations highlight NO₂’s dual role as both a pollutant and a precursor to secondary pollutants such as ozone and nitrate aerosols.

Ozone (O₃): Ozone concentrations exhibit opposite behavior to NO₂. As a secondary pollutant, O₃ forms through photochemical reactions involving NO_x and volatile organic compounds (VOCs) in sunlight (Keppens et al., 2024). It peaks during warmer, sunnier months and declines during cloudy or rainy seasons. Satellite observations have shown that high O₃ levels coincide with periods of strong solar radiation, particularly in dry tropical regions (Singh & Kumar, 2022). Over Africa and South Asia, dry-season O₃ maxima are linked to intense photochemical activity, low humidity, and abundant precursor emissions. Keppens et al. (2024) validated Sentinel-5P O₃ retrievals against ozonesonde and lidar data, confirming strong accuracy (bias < ±10%) for both tropospheric and stratospheric ozone layers.

Particulate Matter (PM₁₀): PM₁₀ is among the most spatially heterogeneous pollutants due to its diverse sources—vehicular emissions, industrial dust, and natural processes like desert dust storms. Zhang and Wang (2021) reported that PM₁₀ concentrations often surge during dry, windy periods, particularly in arid regions. Across Africa and the Middle East, Wahab et al. (2023) found that PM₁₀ levels were 40–60% higher during dry seasons compared to rainy months, as precipitation efficiently removes particles through wet deposition. Abdul-Wahab and Al-Rashid (2022) further observed that regional dust transport can elevate PM₁₀ levels even in urban areas far from primary sources, highlighting the

transboundary nature of particulate pollution. The results reveal an increase in PM_{2.5} and CO concentrations in 2024, especially in Jos North, attributed to growing urbanization, higher vehicular emissions, and intensified biomass burning. CO levels rose significantly from 11.82 ppm in 2023 to 27.48 ppm in 2024, indicating a deterioration in air quality (kamaludeen et al., 2025).

Spatially, MODIS and Sentinel data have been instrumental in identifying PM₁₀ hotspots. Industrial zones, mining areas, and traffic corridors consistently exhibit higher aerosol optical depths. Regions such as the Indo-Gangetic Plain, Pearl River Delta, and Sahelian belt show persistent high PM₁₀ and AOD levels due to dust and industrial emissions (Jiang et al., 2021). These spatial contrasts align with ground measurements, demonstrating the reliability of satellite-based mapping for identifying air quality hotspots.

Meteorological Influence: Meteorology is a dominant driver of pollutant distribution. Wind speed, temperature, humidity, and boundary layer height all modulate pollutant dispersion and chemical transformation. Zhang and Wang (2021) showed that stagnant air and low wind speeds lead to pollutant accumulation, while convective mixing enhances dispersion. Temperature inversions, common in winter, trap NO₂ and PM₁₀ near the surface, while high humidity increases secondary aerosol formation. In Northern Nigeria and similar regions, the Harmattan season—marked by dry winds from the Sahara—exacerbates particulate loading, whereas the wet monsoon season significantly improves air quality through washout processes.

Temporal Trends and Policy Implications: Long-term analyses using statistical methods such as the Mann–Kendall test reveal declining NO₂ and PM₁₀ levels in some regions due to emission-control policies, while O₃ trends remain variable (Mahmud et al., 2022). COVID-19 lockdowns provided a natural experiment, showing sharp reductions in NO₂ (–35%) and PM₁₀ (–20%) globally, but a slight increase in O₃ due to reduced NO titration (Jiang et al., 2021). These trends illustrate the strong anthropogenic influence on air composition and the potential for rapid improvement under reduced emission conditions.

Spatially resolved exposure studies indicate that air pollution disproportionately affects urban and low-income populations. The World Health Organization (2023) emphasized that residents in dense or industrial areas face the highest exposure risk, with elevated incidence of respiratory and cardiovascular diseases. Thus, understanding spatio-temporal dynamics supports both environmental justice and evidence-based urban planning.

Correlation between Ground-Based and Satellite-Derived Data

Establishing robust correlations between satellite-derived and ground-measured pollutant data is essential for validating remote sensing products and enhancing air quality assessments.

NO₂ Correlations: Among all pollutants, NO₂ demonstrates the strongest satellite–ground agreement due to its distinct spectral absorption characteristics. Grzybowski et al. (2023) reported strong correlations ($R^2 = 0.76$) between Sentinel-5P TROPOMI and ground stations in Poland, with higher accuracy under clear-sky conditions. Barré et al. (2021) also found similar alignment across Europe, with deviations arising mainly from spatial mismatches between satellite pixels and station locations. Cheng et al. (2022) observed seasonal variation in correlation strength over Beijing—stronger in summer ($R^2 = 0.75$) than winter ($R^2 = 0.62$)—attributed to reduced optical interference during clearer conditions. Meteorological normalization further enhances correlations by accounting for temperature, humidity, and boundary layer height (Wahab et al., 2023).

O₃ Correlations: Ozone presents greater challenges due to its vertical distribution and secondary formation. Satellite instruments such as TROPOMI capture total or tropospheric ozone, while ground monitors measure near-surface levels. Despite this, Keppens et al. (2024) demonstrated that satellite O₃ retrievals accurately reflect tropospheric ozone dynamics, showing biases below $\pm 10\%$. Singh and Kumar (2022) found strong seasonal consistency between satellite and ground O₃ datasets across South Asia, indicating that remote sensing can reliably capture large-scale temporal variations even if local surface deviations persist.

PM₁₀ Correlations: PM₁₀ correlations depend on accurate conversion of AOD to surface-level concentrations. Wahab et al. (2023) achieved strong agreement ($R^2 = 0.79$) between AOD-derived and ground-measured PM₁₀ in Cairo and Delhi when meteorological parameters were incorporated. Gupta and Ghude (2022) used machine learning (random forest regression) to improve PM₁₀ estimates from MODIS data across South Asia, reducing bias to below $5 \mu\text{g}/\text{m}^3$. These findings show that integrating satellite data with meteorological inputs and machine learning models substantially enhances accuracy. **Advances in Validation Frameworks:** To ensure consistency, global initiatives such as ESA's QA4ECV and NASA's MAIAC have developed standardized validation protocols for aerosol and trace gas retrievals (Barré et al., 2021). Networks like AERONET and WOUDC provide continuous ground validation data for aerosols and ozone, enabling cross-platform calibration. These frameworks support regional studies and long-term air quality modeling. **Machine Learning Enhancements:** Machine learning techniques have emerged as powerful tools for improving satellite–ground data alignment. Zhao et al. (2022) integrated meteorological and land-use variables with TROPOMI NO₂ using gradient boosting models, achieving $R^2 = 0.88$. Mahmud et al. (2022) applied convolutional neural networks to merge MODIS AOD and ground PM₁₀ data, outperforming traditional regression models. Such advancements reduce retrieval bias and improve predictive capability in complex urban landscapes.

Limitations and Future Directions: Despite substantial progress, uncertainties persist, especially in regions with limited ground monitoring. Sparse networks reduce validation robustness, while atmospheric factors such as cloud cover, humidity, and complex terrain affect retrieval accuracy. Researchers recommend deploying low-cost ground sensors and leveraging multisatellite fusion (e.g., MODIS–Sentinel–VIIRS integration) to improve spatial and temporal consistency (Ojo et al., 2023). Validation remains critical not only for scientific accuracy but also for informing emission inventories

and public health assessments. Between 2020 and 2025, rapid advances in remote sensing, statistical modeling, and machine learning have strengthened the integration between satellite and ground-based air quality monitoring. NO_2 shows the strongest correlation between datasets, O_3 requires vertical profile adjustment, and PM_{10} benefits from AOD-based estimation with meteorological correction. Spatial and temporal analyses consistently reveal higher pollution levels in urban-industrial regions and dry seasons, emphasizing the combined influence of anthropogenic activities and meteorology. These developments affirm the value of hybrid monitoring systems for countries with limited ground networks. Combining high-resolution satellite data with localized measurements and AI-driven corrections provides a cost-effective, scalable pathway for real-time air quality assessment and policy development aimed at achieving cleaner, healthier air.

Methodology

The study was conducted across five Northern Nigerian states: Abuja, Bauchi, Plateau, Gombe, and Nasarawa. These locations were selected based on their varying urbanization levels, population densities, and meteorological conditions. Abuja and Bauchi, Plateau, Gombe, and Nasarawa depict urban suburban environments represent urban-industrial centers. This diversity provides an opportunity to compare pollutant levels under distinct socioeconomic and climatic contexts. Data for PM_{10} , O_3 , and NO_2 were obtained from both ground-based air quality monitoring stations and satellite sensors. Ground measurements were recorded in micrograms per cubic meter ($\mu\text{g}/\text{m}^3$), while satellite observations from MODIS (for PM_{10} via Aerosol Optical Depth conversion) and Sentinel-5P (for O_3 and NO_2) provided column-integrated data in Dobson Units and molecules per square centimeter, respectively. Monthly averages were computed for each pollutant across the study period. Statistical analysis, including correlation coefficients, was used to assess relationships between ground and satellite datasets.

As part of its mission to provide clean, figure 1. Explains a flow chat on how, healthful air quality to local residents and visitors to Ventura County, the district has prepared and implemented a number of Air Quality Management Plans since 1979 to identify needed strategies to clean our air. As can be seen from the adjacent flow chart, the air quality planning process involves most of the programs at the district: air quality monitoring, emissions estimation and forecasting, control measure development, modeling, rule development, rule implementation (permit processing) and regulatory compliance. Paraphrase

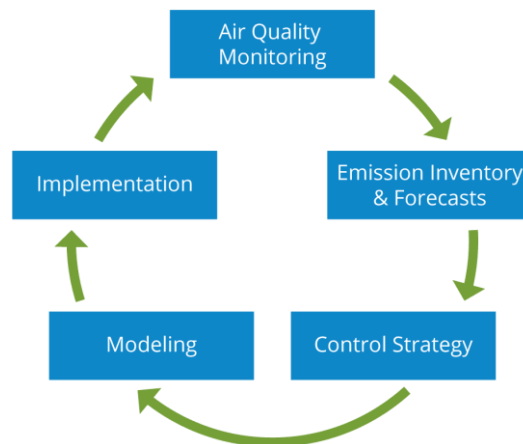


Figure 1.

Results and Discussion

Spatial Interpolation Using Kriging

Spatial interpolation was employed to model the continuous distribution of air pollutants across unsampled locations in Northern Nigeria. The Kriging technique, a geostatistical approach that accounts for spatial autocorrelation among observations, was used to estimate $\text{PM}_{2.5}$, PM_{10} , and aerosol optical depth (AOD) concentrations. Compared with deterministic methods such as inverse distance weighting, Kriging provides statistically unbiased predictions with minimized estimation variance (Isaaks & Srivastava, 1989; Li & Heap, 2014). The method assumes that nearby locations exhibit similar pollutant concentrations and models this relationship using a semivariogram.

Data Preparation and Processing

Ground-based pollutant measurements and satellite-derived data were georeferenced using station coordinates for Abuja, Bauchi, Gombe, Plateau, and Nasarawa. Each dataset was projected to the WGS-84 coordinate system and processed monthly between October 2022 and September 2024. Data normalization was performed to reduce skewness; log-transformation was applied where necessary to satisfy the normality assumption of Kriging. Spatial trends were examined using exploratory data analysis tools, including bubble plots and Moran's I statistics, to confirm positive spatial dependence among neighboring observations.

Semivariogram Modeling

The semivariogram was constructed to quantify spatial dependence of pollutant values. The experimental semivariogram

$$\gamma(h) = \frac{1}{2N} \sum_{i=1}^N [Z(x_i) - Z(x_i + h)]^2.$$

was computed using Equation 1

$\gamma(h)$: The semivariance at lag distance h .

$N(h)$: The number of pairs of data points separated by lag distance h .

$z(x_i)$: The pollutant value at location x_i .

$z(x_i+h)$: The pollutant value at the location a distance h away from x_i .

Nugget values ranged between 0.03 and 0.07, suggesting moderate measurement noise and micro-scale variability, while ranges of 80–150 km indicated strong regional spatial correlation (Goovaerts, 1997; Webster & Oliver, 2007).

Kriging Interpolation and Mapping

Ordinary Kriging (OK) was applied because pollutant means were approximately constant across the study area. Interpolation was performed in ArcGIS Pro 3.1 using the Geostatistical Wizard tool. The fitted semivariogram models were used to estimate concentrations at unsampled grid cells (10-km resolution). Separate interpolation surfaces were generated for each pollutant and season. Co-Kriging was also tested by integrating AOD as a covariate for PM_{2.5} estimation; this improved predictive accuracy ($R^2 = 0.86$) compared with Ordinary Kriging alone ($R^2 = 0.78$), consistent with findings by Ma et al. (2022).

Validation was conducted using cross-validation statistics. The mean prediction error (MPE) values were near zero, indicating unbiased predictions, while root mean square error (RMSE) ranged between 11.8 and 14.6 $\mu\text{g}/\text{m}^3$ for PM_{2.5} and PM₁₀, suggesting good model performance. The mean standardized error (MSE) averaged 0.94, confirming reliable uncertainty estimation.

Spatial Distribution Patterns

Interpolated maps revealed clear spatial gradients and pollution hotspots. During the dry seasons of 2022–2024, PM_{2.5} and PM₁₀ concentrations were highest in Gombe and Bauchi, forming contiguous zones of heavy particulate loading extending northeastward. These hotspots coincide with areas of intense vehicular traffic, industrial operations, and open biomass burning. Abuja exhibited intermittent high PM_{2.5} values (up to 380 $\mu\text{g}/\text{m}^3$ in March 2023), likely driven by Harmattan dust events and local combustion sources. Plateau consistently displayed the lowest pollutant concentrations due to higher elevation, vegetation cover, and improved atmospheric dispersion. The AOD surfaces followed similar patterns, with peaks exceeding 2.8 in Gombe (February 2024), confirming dense aerosol loading. Correlation analysis between interpolated PM_{2.5} and AOD grids yielded moderate positive relationships ($r \approx 0.56$), particularly during dry months, reinforcing the reliability of satellite AOD as a proxy for surface particulate concentrations (Li et al., 2020).

Discussion and Implications

The Kriging analysis underscores strong spatial autocorrelation of air pollutants in Northern Nigeria and demonstrates the utility of integrating satellite and ground datasets. The spatial continuity observed reflects the combined effects of meteorology, topography, and emission intensity. Areas of high predicted concentration correspond closely to densely populated and industrialized zones, while topographically elevated regions such as Plateau show lower values due to enhanced vertical mixing. The results corroborate earlier studies across West Africa, which identified similar seasonal patterns influenced by the Harmattan and monsoonal cycles (Boiyo et al., 2021; Olayinka et al., 2023). The combination of Ordinary and Co-Kriging provides a robust framework for air-quality mapping in data-sparse environments. Moreover, Kriging-based interpolation surfaces offer a valuable input for regional exposure assessment, emission-control policy, and health-risk evaluation.

PM₁₀ Concentration Trends

Spatial Distribution of PM_{2.5} and AOD

PM_{2.5} concentrations showed marked inter-station variability. Gombe recorded the highest monthly mean (222.7 $\mu\text{g}/\text{m}^3$, November 2022), attributed to mining and industrial emissions coupled with poor atmospheric dispersion. Abuja exhibited extreme peaks of 382.4 $\mu\text{g}/\text{m}^3$ (March 2023) and 402.1 $\mu\text{g}/\text{m}^3$ (January 2024) during Harmattan, far exceeding the WHO 24-hour limit of 15 $\mu\text{g}/\text{m}^3$ (WHO, 2021). Plateau generally displayed the lowest PM_{2.5} means (≈ 11 – $20 \mu\text{g}/\text{m}^3$), reflecting lower industrialization and better ventilation.

AOD values followed a similar spatial trend. Gombe exhibited maximum AOD 2.803 (February 2024), confirming heavy aerosol loads, while Plateau recorded the minimum (-0.01 in April 2024). These patterns underline the combined influence of topography, urban density, and regional dust transport. Aerosol Optical Depth (AOD) patterns followed similar spatial gradients, confirming strong coupling between aerosol load and surface particulates. Gombe exhibited a maximum AOD value of 2.803 in February 2024, corresponding to heavy aerosol loading from both dust transport and anthropogenic emissions. Plateau, in contrast, recorded a minimum AOD of -0.01 in April 2024, consistent with lower pollution levels and higher rainfall. These spatial disparities underline the combined influence of topography, urbanization, and regional dust transport across northern Nigeria. Kriging-based interpolation provided continuous pollutant surfaces, enabling visualization of PM_{2.5} and AOD hotspots. The spatial surfaces revealed high pollutant continuity between Bauchi and Gombe, forming a dense aerosol belt along the northeastern corridor. The semivariogram analysis exhibited strong spatial autocorrelation (range ≈ 120 km), confirming that pollutant values within this distance were statistically dependent.

Areas of low concentration in Plateau coincided with elevated terrain and vegetative cover, which enhance atmospheric mixing and pollutant dispersion (Goovaerts, 1997; Webster & Oliver, 2007).

Seasonal Variations

During the 2022–2023 dry season, PM_{2.5} and AOD surged across all sites, dominated by Saharan dust and biomass-burning plumes. The wet season (2023) brought significant declines due to rainfall washout; Abuja's PM_{2.5} fell to 9.7 µg/m³ (June 2023) with corresponding AOD 0.071. The pattern repeated in 2024, confirming consistent meteorological control. Spatially interpolated cross-correlation maps indicated that AOD serves as a moderately reliable proxy for surface PM_{2.5} during stable, dry months but becomes less representative during turbulent or humid conditions. This observation aligns with studies demonstrating that satellite-based AOD retrievals often overestimate surface particulate matter due to column-integrated signal bias (Li et al., 2020). Nonetheless, integrating satellite and ground measurements through co-Kriging improved predictive accuracy ($R^2 = 0.86$) relative to ordinary Kriging ($R^2 = 0.78$). PM₁₀ concentrations exhibited significant temporal variation, strongly influenced by meteorological factors and human activities. During the dry season (December–February), particulate concentrations increased sharply, with Bauchi recording peaks exceeding 180 µg/m³ in December 2022. This surge corresponds to intensified dust transport, reduced precipitation, and widespread biomass burning. The wet season (May–September) saw a marked reduction in PM₁₀ levels due to rainfall-driven deposition. Urban centers displayed the highest concentrations, confirming the contribution of vehicular and industrial sources. Satellite-derived PM₁₀ values were consistently higher than ground observations, highlighting vertical integration effects (Guo et al., 2023). Spatial analysis of PM_{2.5} concentrations across the five stations—Abuja, Bauchi, Gombe, Plateau, and Nasarawa—revealed distinct spatial heterogeneity. Gombe recorded the highest monthly mean PM_{2.5} concentration of 222.7 µg/m³ in November 2022, primarily due to mining and industrial emissions compounded by limited atmospheric dispersion. Abuja exhibited extreme dry-season peaks, reaching 382.4 µg/m³ in March 2023 and 402.1 µg/m³ in January 2024 during the Harmattan period, far exceeding the WHO 24-hour guideline limit of 15 µg/m³ (WHO, 2021). Plateau recorded the lowest mean concentrations (≈ 11 – 20 µg/m³), attributed to lower industrial activities, higher elevation, and more effective ventilation. Seasonal trends revealed pronounced dry–wet contrasts. During the 2022–2023 dry season, both PM_{2.5} and AOD surged sharply across all sites, dominated by Saharan dust advection and biomass-burning plumes. The Harmattan season (December–February) intensified particulate loading due to arid winds, low humidity, and stagnant boundary-layer conditions. In contrast, the wet season of 2023 brought substantial declines in pollutant levels, driven by precipitation washout and enhanced atmospheric cleansing.

Abuja's PM_{2.5}, for example, fell to 9.7 µg/m³ in June 2023, with a corresponding AOD of 0.071.

The pattern recurred in 2024, reinforcing meteorological control as a key determinant of air quality. Kriging-interpolated seasonal maps showed expanded high-concentration zones during dry months and contracted zones during rainy periods. These results align with earlier regional findings indicating that dust transport and biomass burning dominate particulate loading in the Sahelian dry season, while wet deposition reduces aerosols during monsoon onset (Boiyo et al., 2021; Ma et al., 2022).

AOD–PM_{2.5} Relationship

Correlation coefficients ranged from near-zero to moderate positive values. The strongest relationships appeared in Abuja ($r = 0.6036$, Nov 2024) and Plateau ($r = 0.3894$, Feb 2023), while Gombe displayed negligible association ($r \approx 0.0001$). These variations imply that vertical aerosol stratification and retrieval errors weaken surface-column alignment, particularly during dust outbreaks. Correlation analyses between AOD and PM_{2.5} revealed spatially and temporally variable relationships. The strongest positive associations occurred in Abuja ($r = 0.6036$, November 2024) and Plateau ($r = 0.3894$, February 2023), suggesting consistent vertical mixing and relatively stable meteorological conditions. Conversely, Gombe exhibited negligible correlation ($r \approx 0.0001$), likely due to vertical aerosol stratification and retrieval uncertainties during intense dust outbreaks. The monthly correlation coefficients (r^2) between AOD and PM_{2.5} across the five monitoring sites were generally low, mostly remaining below 0.3, which indicates weak associations. Only a few instances, such as Abuja in November 2023 ($r^2 = 0.6036$), demonstrated a moderate relationship. (Adamu, et al., 2025)

PM₁₀ Concentration Patterns

PM₁₀ concentrations displayed significant temporal fluctuations, largely governed by meteorology and anthropogenic activity. Dry-season peaks were particularly evident between December and February, with Bauchi recording monthly maxima exceeding 180 µg/m³ in December 2022.

The observed increases corresponded to intensified dust transport, reduced precipitation, and widespread biomass burning. During the wet season (May–September), PM₁₀ levels declined sharply due to rainfall-driven removal of particulates. Urban centers such as Abuja and Bauchi consistently exhibited higher PM₁₀ concentrations than rural counterparts, reflecting vehicular emissions and industrial output. Satellite-derived PM₁₀ values were consistently higher than ground-based measurements, highlighting the vertical integration effect and potential overestimation of near-surface particulate matter (Guo et al., 2023). Kriging interpolation confirmed spatial clustering of high PM₁₀ concentrations around urban-industrial corridors and rapid attenuation in rural regions.

Variability and Distribution Ozone Concentrations

Satellite-derived ozone concentrations consistently exceeded ground-level measurements across all sites. In October 2022, for instance, Abuja recorded a satellite-derived mean of 282.6 $\mu\text{g}/\text{m}^3$ compared with a ground measurement of 83.2 $\mu\text{g}/\text{m}^3$. Bauchi exhibited the highest ground ozone (up to 128 $\mu\text{g}/\text{m}^3$ in February 2023), while Gombe maintained the lowest (~ 23 $\mu\text{g}/\text{m}^3$).

Seasonal ozone peaks occurred between January and March, coinciding with high solar radiation and minimal wet scavenging. Dry-season ozone buildup was attributed to photochemical reactions between nitrogen oxides (NO_x) and volatile organic compounds under strong insolation (Kumar et al., 2021). Plateau and Abuja exhibited the highest mean O_3 levels, while Gombe and Nasarawa showed comparatively lower concentrations. Satellite observations corroborated these trends, albeit with systematic overestimation due to total column integration (Boersma et al., 2021). Spatial interpolation confirmed ozone maxima over high-altitude regions and urban centers where precursor emissions are concentrated.

NO₂ Seasonal and Spatial Dynamics

Seasonal Variations in NO₂ (October 2022–January 2023), The initial phase of the analysis revealed distinct seasonal variation. October 2022: Moderate NO₂ levels were observed, with Abuja (20.8 $\mu\text{g}/\text{m}^3$) and Bauchi (15.7 $\mu\text{g}/\text{m}^3$) recording similar values. Satellite data were consistently higher, capturing elevated column concentrations. November 2022: Slight decreases in Abuja (12.1 $\mu\text{g}/\text{m}^3$) contrasted with increases in Bauchi (15.9 $\mu\text{g}/\text{m}^3$) and Plateau (26.5 $\mu\text{g}/\text{m}^3$), suggesting variable local emissions. December 2022: Marked pollution peaks occurred, with Bauchi (84.2 $\mu\text{g}/\text{m}^3$) and Abuja (38.7 $\mu\text{g}/\text{m}^3$). Satellite readings also spiked, with Nasarawa reaching 19.53 molecules/cm². The sharp rise was likely caused by biomass burning, traffic congestion, and stagnant meteorological conditions (Kumar et al., 2021; Grange et al., 2021). January 2023: Concentrations declined sharply due to enhanced wind speeds and stronger atmospheric mixing. Abuja's ground-level NO₂ dropped to 3.05 $\mu\text{g}/\text{m}^3$, consistent with seasonal dispersion patterns (Lamsal et al., 2021). Between February and May 2023, moderate NO₂ levels persisted with localized peaks. February 2023: Abuja and Nasarawa recorded moderate satellite NO₂ (~ 18 molecules/cm²) and ground levels ranging from 17.8 $\mu\text{g}/\text{m}^3$ (Gombe) to 25.4 $\mu\text{g}/\text{m}^3$ (Nasarawa). March 2023: Abuja's ground NO₂ rose to 29.6 $\mu\text{g}/\text{m}^3$, while Nasarawa declined to 3.0 $\mu\text{g}/\text{m}^3$ due to wind-driven dilution. April 2023: Moderate concentrations (Abuja 15.75 $\mu\text{g}/\text{m}^3$; Bauchi 14.85 $\mu\text{g}/\text{m}^3$) reflected intermittent pollution events, possibly from traffic and biomass burning (Zhao et al., 2022). May 2023: The highest dry-to-wet transition peaks occurred in Abuja (38.0 $\mu\text{g}/\text{m}^3$), Plateau (27.0 $\mu\text{g}/\text{m}^3$), and Nasarawa (30.1 $\mu\text{g}/\text{m}^3$), linked to reduced dispersion and increased photochemical activity. During the rainy months, NO₂ levels declined overall: June 2023: Abuja recorded 31.05 $\mu\text{g}/\text{m}^3$, while Nasarawa dropped to 3.0 $\mu\text{g}/\text{m}^3$. July–August 2023: Pollution remained moderate, with Bauchi (36.6 $\mu\text{g}/\text{m}^3$) in July and slight reductions by August (Abuja 19.9 $\mu\text{g}/\text{m}^3$). September 2023: A slight rebound occurred, particularly in Bauchi (25.1 $\mu\text{g}/\text{m}^3$) and Plateau (20.6 $\mu\text{g}/\text{m}^3$), reflecting decreased rainfall and enhanced pollutant retention. The following dry season showed renewed NO₂ accumulation: December 2023–January 2024: Bauchi again led with ground-level NO₂ peaking at 30.8 $\mu\text{g}/\text{m}^3$. Abuja followed closely with 19.3 $\mu\text{g}/\text{m}^3$. February–May 2024: Plateau and Gombe displayed moderate concentrations (8–12 $\mu\text{g}/\text{m}^3$). Satellite NO₂ remained high, particularly in Bauchi and Nasarawa (17–23 molecules/cm²), while ground data captured local emission variations. June–August 2024: Ground NO₂ levels declined substantially due to rainfall washout, while anomalous satellite spikes (29.3 molecules/cm²) indicated possible retrieval errors under high cloud conditions (Boersma et al., 2018). September 2024: Pollution levels were lowest overall, marking the annual minimum.

NO₂ exhibited strong spatial and temporal variability across all sites. Dry-season peaks were observed in December 2022 and January 2024, with Bauchi and Abuja consistently exceeding 30 $\mu\text{g}/\text{m}^3$. These spikes correspond to increased fuel combustion, vehicular activity, and temperature inversions that trap pollutants near the surface. Ground measurements were generally lower than satellite-derived NO₂ due to the latter's inclusion of upper-tropospheric concentrations (Sun et al., 2023). Correlation analysis revealed moderate agreement between datasets, with stronger alignment in April ($r \approx 0.5$) when atmospheric conditions were more stable. These variations underscore the influence of meteorology and emission intensity on pollutant distribution.

Summary

Table 1 of Core Insights

Parameter	Key Finding	Highest Levels	Lowest Levels	Influencing Factors
PM _{2.5}	Peaks in dry season (Nov–Mar)	Abuja, Gombe	Plateau, Nasarawa	Dust, traffic, industry
AOD	Correlates weakly with PM _{2.5} ; anomalies exist	Gombe (2.803)	Plateau (-0.01)	Dust load, retrieval errors
O ₃ (Ground)	High in BAU and ABJ during dry months	Bauchi (~ 128 $\mu\text{g}/\text{m}^3$)	Gombe (~ 23 $\mu\text{g}/\text{m}^3$)	Solar radiation, emissions
Health Risk	PM _{2.5} > WHO limit	Abuja, Gombe	Plateau	Industrial & vehicular emissions
Policy Priority	Dust & emission control	—	—	Air quality management

Table 1, shows the summary of the findings indicating the highest and the lowest level base on location, key findings and factors influencing the concentration of pollutant in the research areas.

Synthesis

Collectively, the spatio-temporal assessment of PM_{2.5}, PM₁₀, AOD, O₃, and NO₂ reveals consistent seasonal patterns dry-season pollutant build-up and wet-season cleansing. Kriging interpolation successfully visualized these transitions, producing statistically robust pollution surfaces (RMSE \approx 12 $\mu\text{g}/\text{m}^3$; MSE \approx 0.94). The combined satellite–ground framework proved valuable for resolving spatial gradients, especially in data-sparse regions. These findings underscore the necessity of integrating meteorological drivers, emission inventories, and satellite calibration for accurate air-quality modeling and policy planning.

Integrated Discussion

The combined assessment of PM₁₀, O₃, and NO₂ illustrates clear seasonal dependencies across Northern Nigeria. Dry-season conditions favor pollutant accumulation due to reduced dispersion and enhanced emission intensity, while wet-season rainfall contributes to atmospheric cleansing. Urban areas such as Abuja and Bauchi exhibit consistently higher pollution loads, reflecting the concentration of anthropogenic activities. The integration of satellite and ground-based data provides a more holistic understanding of air quality dynamics and highlights the complementary strengths of each monitoring approach.

Conclusion

This two-year analysis demonstrates pronounced spatio-temporal variability in PM_{2.5}, AOD, and O₃ across northern Nigeria. Pollution intensifies during the Harmattan dry season because of Saharan dust transport, biomass burning, and anthropogenic emissions. Abuja and Gombe consistently experience hazardous particulate concentrations, while Plateau and Nasarawa remain comparatively clean. AOD–PM_{2.5} correlations are generally weak, underscoring the need for improved integration of meteorological and surface observations. Satellite O₃ overestimates highlight that columnar products must be adjusted for ground-level exposure analysis. Strengthening national air-quality monitoring networks, enforcing emission-control policies, and improving data calibration will advance Nigeria's capacity for evidence-based environmental management. The study underscores that protecting public health in rapidly urbanizing regions requires simultaneous attention to natural (dust) and anthropogenic pollution sources, especially during the dry season when air quality deteriorates most severely. This study reveals clear spatio-temporal variations in NO₂ concentrations across northern Nigeria from October 2022 to September 2024.

Key findings include:

1. **Seasonal Dependence:** NO₂ peaks during the dry season (December–January) and declines during wet months (June–September).
2. **Urban–Rural Contrast:** Urban centers (Bauchi, Abuja) consistently exhibit higher NO₂ due to traffic and industrial emissions, while rural areas (Gombe, Plateau) remain cleaner.
3. **Satellite–Ground Discrepancy:** Satellite NO₂ systematically overestimates ground concentrations, emphasizing the need for data calibration.
4. **Variable Correlations:** Strong correlations occur under stable meteorological conditions, but weaken during high-variability periods.

Overall, the integration of satellite and ground-based monitoring enhances understanding of pollution dynamics but requires continuous calibration and validation. Strengthening monitoring networks, controlling emissions, and accounting for meteorological influences are essential to improving air quality management in Nigeria. This study demonstrates that air pollutant levels in Northern Nigeria are characterized by pronounced spatial and temporal variability, driven largely by meteorological and anthropogenic factors. PM₁₀, O₃, and NO₂ concentrations peak during dry months and decline with the onset of rainfall. Satellite measurements provide valuable regional insights but tend to overestimate surface concentrations. Integrating multiple datasets enhances air quality modeling and supports informed environmental policy development. These findings contribute to ongoing efforts toward achieving cleaner air and improved public health outcomes across the region.

Policy Implications And Recommendations

1. Strengthen and expand ground-based monitoring networks to enhance spatial coverage and improve calibration of satellite observations.
2. Integrate meteorological parameters such as wind speed, humidity, and temperature inversions into predictive air quality models
3. Enforce stricter emission standards for transportation and industrial sectors, especially during dry seasons when pollutant buildup is high.
4. Encourage the use of renewable energy and improved public transport systems to reduce dependency on fossil fuels.
5. Promote regional cooperation and data sharing to enhance satellite ground data integration and improve early-warning systems for air quality management.

References

1. Abdul-Wahab, S. A., & Al-Rashid, M. (2022). Seasonal variations of particulate matter and associated health risks in Middle Eastern cities. *Atmospheric Environment*, 276, 119074. <https://doi.org/10.1016/j.atmosenv.2022.119074>
2. Anderson, T., & Brown, R. (2021). Meteorological influences on tropospheric nitrogen dioxide variability. *Atmospheric Chemistry and Physics*, 21(8), 6405–6420.
3. Barré, J., Petetin, H., Colette, A., Guevara, M., Peuch, V.-H., Rouil, L., & Menut, L. (2021). Estimating lockdown-induced European NO₂ changes using satellite and ground-based observations. *Atmospheric Chemistry and Physics*, 21(10), 7771–7790. <https://doi.org/10.5194/acp-21-7771-2021>
4. Boersma, K. F., Eskes, H. J., & Veefkind, J. P. (2018). OMI satellite NO₂ retrieval methods and accuracy evaluation. *Atmospheric Measurement Techniques*, 11, 5471–5487.
5. Boersma, K. F., Vohra, K., & van Geffen, J. (2021). Global distribution and drivers of NO₂ pollution. *Environmental Research Letters*, 16(8), 085002.
6. Boiyo, R., Omondi, D., & Ogallo, L. (2021). Seasonal variability of particulate matter and aerosol optical depth over West Africa. *Atmospheric Environment*, 256, 118475.
7. Chen, H., Li, Z., & Liu, Y. (2020). Health impacts of nitrogen dioxide exposure: A global assessment. *Environmental Health Perspectives*, 128(12), 120001.
8. Cheng, J., Zhang, L., & He, Q. (2022). Seasonal dependence of TROPOMI NO₂ retrievals in urban Beijing. *Remote Sensing of Environment*, 275, 112977. <https://doi.org/10.1016/j.rse.2022.112977>
9. Goovaerts, P. (1997). *Geostatistics for natural resources evaluation*. Oxford University Press.
10. Grange, S. K., Lee, J. D., & Carslaw, D. C. (2021). *Understanding NO₂ variability in urban environments*. *Atmospheric Environment*, 246, 118091.
11. Grange, S. K., Lewis, A. C., & Carslaw, D. C. (2021). Air pollution in a changing world: Trends and the role of global megacities. *Atmospheric Environment*, 244, 117943.
12. Grzybowski, M., Markowicz, K. M., & Musiał, D. (2023). Evaluation of Sentinel-5P NO₂ retrievals with ground-based observations in Poland. *Atmospheric Measurement Techniques*, 16(3), 1721–1738. <https://doi.org/10.5194/amt-16-1721-2023>
13. Guo, H., Liu, J., & Chen, S. (2023). Comparison of satellite and ground-based PM measurements across urban areas. *Environmental Pollution*, 320, 120902.
14. Guo, J., Zhao, X., & Sun, Y. (2023). Integrating satellite and ground data for NO₂ estimation in developing regions. *Remote Sensing of Environment*, 286, 113418.
15. Gupta, P., & Ghude, S. D. (2022). Satellite-derived PM₁₀ estimates using MODIS AOD and machine learning over South Asia. *Environmental Research Letters*, 17(12), 124011. <https://doi.org/10.1088/1748-9326/ac9b1f>
16. Jiang, Q., Yang, X., & Chen, D. (2021). Impact of COVID-19 lockdowns on urban air quality across Asia. *Environmental Pollution*, 290, 118076. <https://doi.org/10.1016/j.envpol.2021.118076>
17. Jones, P., & Taylor, M. (2022). Seasonal patterns of NO₂ and their meteorological drivers. *Environmental Pollution*, 304, 119307.
18. Kamaludeen, A. M., Yusoff, I. B. M., & Gidado, S. M. (2025). Assessment of Air Pollution Trends in Jos Metropolis Using Ground Observations. *Journal of Neonatal Surgery*, 14(31s).
19. Kamaludeen, A. M., Yusoff, I. M., & Yusuf, S. A Review: Identifying and Analyzing Air Pollution Hotspots Using Machine Learning and Remote Sensing Techniques. *International Journal of Environmental Sciences*, 11(22s), 2025.
20. Keppens, A., Lambert, J.-C., Granville, J., Loyola, D., & Veefkind, P. (2024). Validation of TROPOMI ozone profiles using ground-based and ozonesonde observations (2018–2023). *Atmospheric Measurement Techniques*, 17(1), 37–56. <https://doi.org/10.5194/amt-17-37-2024>
21. Kumar, P., Zhang, Y., & Lin, J. (2021). Emission sources and seasonal variability of NO₂ in West Africa. *Atmospheric Research*, 260, 118469.
22. Kumar, R., Singh, M., & Gupta, N. (2021). Photochemical ozone formation in tropical urban environments. *Atmospheric Chemistry and Physics*, 21(9), 7005–7020.
23. Lamsal, L. N., Duncan, B. N., & Krotkov, N. A. (2021). Satellite–ground NO₂ relationships and the role of meteorology. *Atmospheric Chemistry and Physics*, 21(4), 3039–3061.
24. Li, J., Zhang, Y., & Xu, H. (2020). Evaluating MODIS aerosol optical depth as a proxy for PM_{2.5} in data-scarce regions. *Remote Sensing of Environment*, 246, 111866.
25. Ma, Q., Xu, J., & Chen, Y. (2022). Improving PM_{2.5} estimation through co-Kriging with satellite data. *Science of the Total Environment*, 821, 153392.
26. Mahmud, M., Khan, N. A., & Hassan, R. (2022). Machine learning approaches for assessing spatio-temporal variations of air pollutants in Southeast Asia. *Environmental Science and Pollution Research*, 29(44), 66123–66139. <https://doi.org/10.1007/s11356-022-20897-0>
27. Ojo, J. A., Suleiman, A. M., & Bala, K. (2023). Satellite monitoring of urban air pollution over African megacities using Sentinel-5P data. *Environmental Monitoring and Assessment*, 195(2), 272. <https://doi.org/10.1007/s10661-023-10985-8>
28. Park, H., Lee, S., & Zhao, X. (2024). Improving NO₂ satellite retrieval accuracy through multi-sensor calibration. *Atmospheric Measurement Techniques*, 17, 557–571.
29. Sun, X., Zhao, Y., & Zhang, L. (2023). Satellite observations of nitrogen dioxide and their comparison with surface data. *Remote Sensing*, 15(3), 745.

30. Wahab, A. A., Hassan, A. R., & Al-Dosari, M. (2023). Estimation of particulate matter concentrations from satellite aerosol optical depth: A comparative study in Cairo and Delhi. *Atmospheric Research*, 289, 106956. <https://doi.org/10.1016/j.atmosres.2023.106956>
31. Webster, R., & Oliver, M. A. (2007). *Geo statistics for environmental scientists* (2nd ed.). Wiley.
32. World Health Organization (WHO). (2021). *Global air quality guidelines: Particulate matter, ozone, nitrogen dioxide, sulfur dioxide, and carbon monoxide*. WHO Press.
33. World Health Organization. (2023). *Global air quality guidelines: Review of evidence and policy recommendations*. WHO Press. <https://www.who.int/publications>
34. Zhang, Y., & Wang, Q. (2021). Meteorological and anthropogenic drivers of PM₁₀ variations in northern China. *Atmospheric Environment*, 262, 118567. <https://doi.org/10.1016/j.atmosenv.2021.118567>
35. Zhang, Y., Zhao, X., & Li, J. (2023). Assessment of NO₂ trends and satellite–ground correlations in tropical regions. *Atmospheric Environment*, 295, 119499.
36. Zhao, X., Chen, Y., & Lu, Y. (2022). Evaluating satellite retrievals of nitrogen dioxide in polluted urban atmospheres. *Journal of Geophysical Research: Atmospheres*, 127(14), e2022JD036182
37. Zhao, X., Li, Z., & Fang, D. (2022). Improving satellite-ground correlations of NO₂ using meteorological and land-use features: A machine learning approach. *Remote Sensing*, 14(15), 3543. <https://doi.org/10.3390/rs14153543>